

Exploring the Limits of the Safe Operation Area of Power Semiconductor Devices

(Invited Paper)

C. Sandow, R. Baburske, F.-J. Niedernostheide, F. Pfirsch
Infineon Technologies
Am Campeon 1-12, D-85579 Neubiberg, Germany
Email: ChristianPhilipp.Sandow@infineon.com

C. Töchterle
Institute for Physics of Electrotechnology
Technische Universität München
Arcisstraße 21, D-80333 Munich, Germany

Abstract—TCAD simulations of power devices are an important tool to investigate destruction mechanisms of power diodes and IGBTs. It is found that the dynamics of filamentation is the key for understanding the limits of the safe operation area. For both diodes and IGBTs, destructive and non-destructive filamentation mechanisms are identified and the resulting destruction mechanisms are discussed.

I. INTRODUCTION

Energy efficiency and sustainability are global trends which act as key drivers for the development of future power semiconductor devices. The resulting development targets are a reduction of power losses and a shrink of the footprint by increasing the power density. These goals can be achieved for example by raising the maximum junction temperature, but in this process more and more effort is required to maintain a large safe operating area (SOA). Thus, besides improving the performance, reliability and ruggedness are important design objectives which are ensured by dedicated TCAD simulations and experimental studies. In many cases when exploring the limits of the SOA, the validity range of the physical simulation models are exceeded, e.g. for very high current densities and high carrier densities, large electric fields, strong impact ionization and self-heating effects. In this contribution, we will focus on the limits of the SOA and present simulation results on different destruction mechanisms of power diodes and integrated gate bipolar transistors (IGBT). Beginning from the final state, the destroyed device, we will follow the chain of events that lead to the destruction until we. This discussion will include SOA-failures of power diodes and failure during the turn-off of IGBTs. A general discussion of failure mechanisms can be found in [1] and a more detailed overview on device simulations of failure mechanisms can be found in [2].

II. THE MECHANISM LEADING TO DESTRUCTION

The main mode of SOA failures is destruction by melting parts of the device (for example the metallization). Usually, melting is a result of a large local power dissipation, which is due to very high local current densities (typically several thousand A/cm²). Common nominal power densities of IGBTs and power diodes are below 1000 A/cm². Hence, to reach current densities which are necessary for destruction, the current distribution in the power device needs to be highly inhomogeneous. Such current distributions are commonly caused by filamentation, i.e. small localized regions to which the formerly

homogeneous flow of current concentrates. Yet, the formation of filaments does not necessarily lead to the destruction of the power device. Filaments become destructive only if they deposit enough energy at a certain location, meaning high power density over a long enough time period. In IGBTs, strong filamentation can also trigger latch-up, which will inevitably cause destruction.

One example for the appearance of non-destructive filaments is the turn-off behavior of IGBTs. IGBTs consist of a large array of repeated unit cells which supply current through their MOS-channels. During turn-off, at some point, the carrier plasma in the drift-zone is partly removed and the vertical current flow in the high-field region focuses to areas below the end of the channel. This inhomogeneity of the current flow is due to the structuring of the IGBT cells and is temporary and stable which means that the initial filaments do not concentrate to a smaller number of filaments with higher current densities if the turn-off is performed inside the SOA.

Destructive filaments can occur during several operating conditions in power diodes [3]–[5] and IGBTs [6]–[11]. For example, destructive filaments can appear during unclamped inductive switching, short-circuit operation, over-current turn-off and failures due to cosmic ray irradiation. Mostly, they arise at high voltages and are either a result of inhomogeneous impact ionization rates across the device or of inhomogeneous temperature distributions leading to local thermal runaway. As impact ionization reduces with increasing temperature, it is specific to the impact ionization type of filaments that they can perform a thermal movement. As soon as the primary region of impact ionization heats up significantly, impact ionization reduces locally and the filament moves laterally to an adjacent colder location. Due to the possibility of filament movement, the time evolution of the filaments is important to decide if a filament will become destructive. Sometimes, filament movement can prevent destruction because the energy deposition at a specific position stays too small to destroy the device (e.g. anode-side filamentation during power diode turn-off). In other cases, the movement is too slow or the power density of a filament is very high (e.g. during IGBT latch-up or in cosmic ray events). Under special conditions, filaments merge which results in an increasing power density in the remaining filaments and if this process continues, it can lead to destruction.

Therefore, an important step to understand destruction is

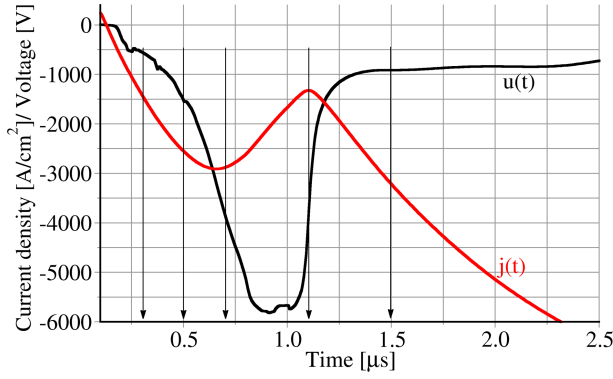


Fig. 1. Simulated diode voltage $u(t)$ and current density $j(t)$ [= $i(t)$ normalized to the diode contact area] during the reverse-recovery process of a diode with low emitter efficiency of the $n+$ region and a blocking capability of 8 kV. (From [2]).

to analyze the formation and evolution of filaments in specific cases. As first example, we discuss the SOA of power diodes [2], [12].

III. POWER DIODE TURN-OFF

High-voltage power devices usually contain a lowly n -doped drift region, which during the on-state is flooded with an electron-hole-plasma. The plasma ensures a low forward voltage drop, but during turn-off the plasma is removed and a high-field region forms across the $p+/n$ -junction. A large current of holes originating from the plasma flows towards the anode and further increases the electric field peak. Under these conditions, impact ionization takes place and can lead to anode-side filaments. These anode-side filaments are electrically self-limiting, because the generated electrons reduce the electric field strength in the filament. This reduced electric field leads to an enhanced local plasma extraction in the filament which results in a fast lateral movement of the filament thus preventing local hot spots. It was shown that the experimental destruction limit correlates with the limit at which impact ionization becomes significant at the $n^- - n^+$ -junction at the backside of the diode. Device simulations indicate that those filaments can be destructive because they only move slowly due to the mentioned thermal mechanism. An in-depth analysis of the plasma dynamics explains the difference between cathode and anode-side filaments [12].

For the 2D simulation of diode destruction, the diode is turned off under extreme switching conditions which exceed the experimental ones. As filamentation is inherently a 3D phenomenon, the 2D simulation is performed at higher current densities to yield comparable current densities in resulting filaments. For example, turn-off can be simulated from a very high current level using an ideal switch which allows a large dI/dt . To prevent an early snappy behavior, which would eventually prevent cathode-side filaments, an additional resistor R is introduced in the mixed-mode simulation.

Fig. 1 shows a simulated diode turn-off with a thermal runaway of the current beginning at $1.1 \mu\text{s}$. The time evolution of the filaments during the switching process is shown in Fig. 2. The electron distribution is plotted at 5 different times which are marked by the arrows in Fig. 1. Initially (at $0.3 \mu\text{s}$), two

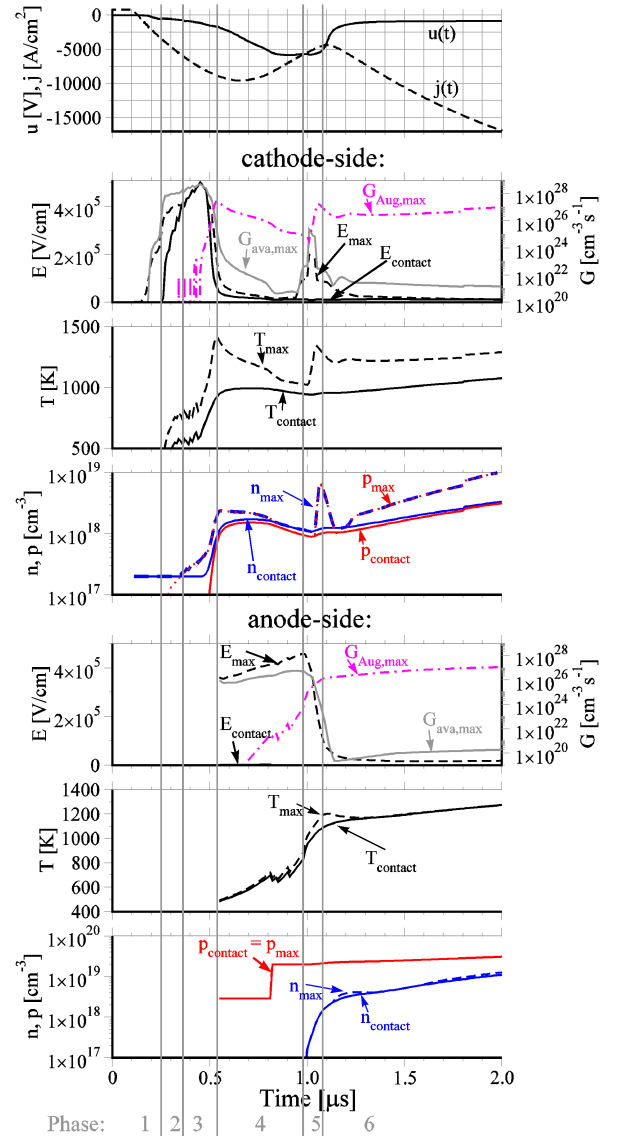


Fig. 3. Reverse-recovery behavior and temporal behavior of several internal variables in the cathode-side and anode-side filament during the reverse-recovery process (Fig. 1). (From [2]).

filaments, one at the cathode and one at the anode are visible, and both are separated by a plasma layer. In the next two snapshots at $0.5 \mu\text{s}$ and $0.7 \mu\text{s}$, the plasma is further removed, the anode-side filament moves and additional filaments form. At the cathode side, the filament does not move and the carrier density within the filament increases dramatically. At $1.1 \mu\text{s}$ the plasma layer disappears and the cathode filament merges with an anode filament leading to a continuous filament at $1.5 \mu\text{s}$. The understanding of this process can be refined by studying the time evolution of several internal variables in six phases (Fig. 3). In the first phase, the reverse current density increases strongly thus leading to the formation of an avalanche driven cathode side filament at about $0.24 \mu\text{s}$. In the second phase, the increase of the maximum hole density at the cathode-side reflects the rising carrier density inside the cathode-side filament. During this process, the electric field (E) increases and its peak moves towards the cathode contact.

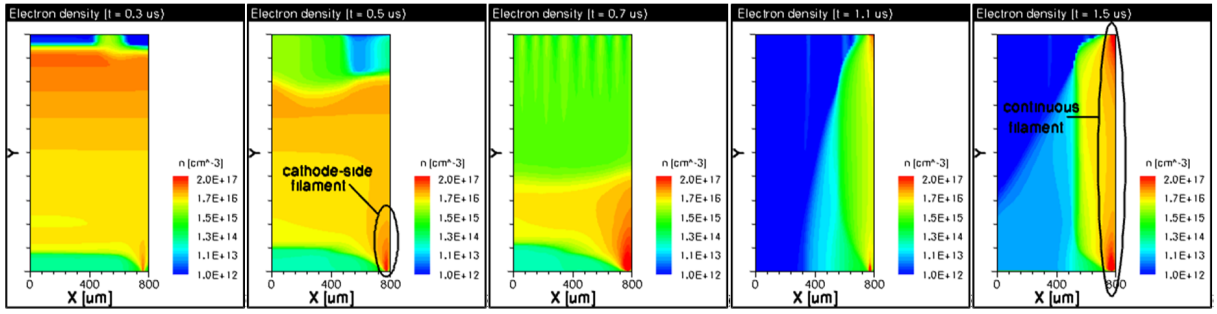


Fig. 2. Electron density during reverse-recovery process at certain points in time marked in Fig. 1 (top ($y = 0$): anode, bottom ($y = d$): cathode, for the left and the right homogeneous Neumann boundary conditions are assumed). (From [2]).

This means that the n^+ -region is punched through. In the third phase, the large power dissipation leads to a rapid increase of the temperature at the contact. At such high temperatures, the impact ionization generation (G_{ava}) decreases but at the same time, the increasing thermal injection at the contact starts to sustain the filament. In addition, the usually neglected thermal Auger generation (G_{Aug}) becomes important because above 1000 K the intrinsic carrier density n_i starts to exceed the product of the carrier densities np . Due to the high carrier densities in the filament, the electric field reduces at the same time. In phase four, the remaining plasma is removed from the anode side with the exception of the region above the cathode-side filament. Moreover, the anode-side filaments vanish with the exception of the filament which is on the opposite side of the cathode-side filament. The large carrier density inside the cathode-side filament expands towards the anode and reduces the depletion layer width at its position. At the end of phase four, both filaments merge and in phase five, the filament at the anode side turns from an impact ionization driven filament into a thermally driven filament as well. Eventually, in phase six a positive feedback between both thermal filaments leads to thermal runaway and the destruction of the chip.

This analysis illustrates the general destruction mechanism, though it has been shown that if cathode-side filaments appear very late during turn-off, they do not always cause chip destruction. Nevertheless, this analysis helps to identify the $n^+ - n^-$ junction playing a critical role during destruction and helps to improve the ruggedness of power diodes [14]. But, to achieve a better quantitative agreement with experimental results, further effort is needed for improving physical models and performing numerically expensive 3D-simulations.

IV. IGBT OVERCURRENT TURN-OFF

A second example of filament formation and dynamics is during the overcurrent turn-off of a trench-IGBT [14], [15]. For these simulations, a monolithic IGBT is divided into two parts: A first part which represents a variable amount of IGBT cells in one simulation mesh and a second part which contains one scaled IGBT cell and represents the remaining chip area that carries most of the current during the on-state of the device. Both parts are arranged in a parallel configuration using a mixed-mode simulation setup. Initially, the gate voltage of the IGBT is biased to a rather high voltage in order to allow a significant overcurrent to flow without desaturation of the plasma. Then, the IGBT is turned off with an inductive load, a given stray inductance and a typical gate resistance.

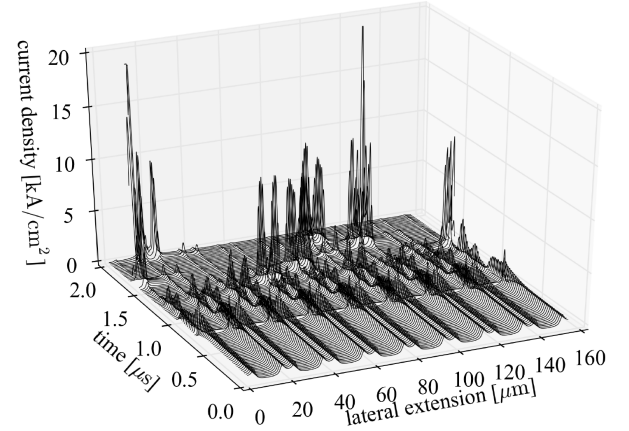


Fig. 4. Electric current density underneath the trenches as a function of. The evolution of moving current filaments in a 16-IGBT monolithic structure during turn-off with no latch-up. The initial current density is 400 A/cm^2 . (From [15])

Depending on whether the initial current is above or below a certain threshold, the device is either destroyed or remains functional.

The dynamics of the filament formation for non-destructive filaments is shown in Fig. 4. Even in the on-state of the device (at $t = 0$), a certain inhomogeneity of the current flow exists because electrons flow through the MOS-channels and are locally emitted into the drift zone. As soon as the MOS-channels are closed (at $t = 1.0 \mu\text{s}$), impact ionization at the trench bottom becomes dominant and numerical variations cause fluctuations of the current densities. At $t = 1.5 \mu\text{s}$, stronger filaments become apparent, but they are electrically self-limited and move around similar to anode-side filaments in diodes.

An important observation is that the number of filaments during turn-off reduces and at the same time, the current density within the remaining filaments increases. This behavior might be a result of the shrinking plasma layer during turn-off which can homogenize the current distribution only if it has a significant vertical extent. For larger initial currents, the maximum current density in the filaments will increase. We observe that, as soon as the hole current density at the emitter contact corresponding to a filament exceeds 1000 A/cm^2 (Fig. 5), another effect starts to amplify the filament current. In the IGBT, hole current flows close to the n^+ -doped emitter region. But, if the hole current density is very large, a

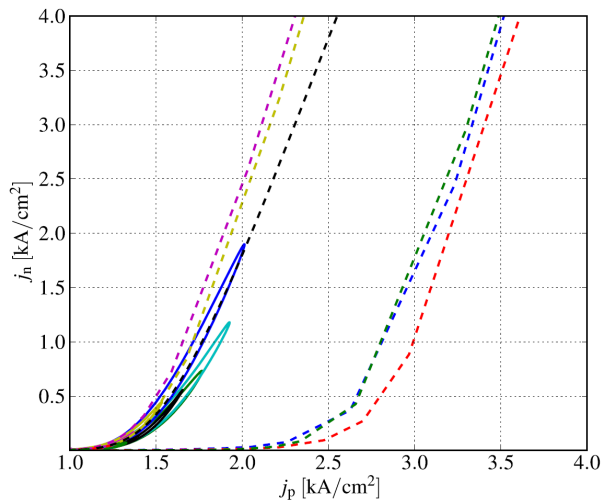


Fig. 5. Electron current density as a function of the hole current density for the emitter contacts of each cell in a 16-cell monolithic structure. The dashed lines show the latching cells. The initial current density is 500 A/cm^2 which is just above the latch-up threshold. The threshold for significant electron current is at a hole current of 1 kA/cm^2 . A second threshold at 2 kA/cm^2 exists for cells which are direct neighbors of latching cells. (From [15])

voltage drop builds up along the n^+/p -body junction and if this voltage drop starts to compensate the built-in potential of the junction, electrons are emitted into the p-body. If this electron current becomes significantly large, latch-up will occur and will lead to destruction because of its positive feedback. In a comprehensive simulation study, the impact of the number of monolithically integrated cells as well as the influence of isothermal vs. electro-thermal simulations was studied [15]. It was found that the total current density at which latch-up occurs depends on the number of cells, but saturates above 20 cells (see Fig. 6). Moreover, in electro-thermally coupled simulations, the latch-up threshold is comparable to isothermal simulations.

Though the simulations are not yet fully quantitative, the presented methodology enables the optimization of future device concepts.

V. CONCLUSION

Device simulations are a very important tool to understand failure mechanisms and to identify ways for optimization. To illustrate this, two examples for the destruction mechanisms of power devices during turn-off are discussed. In both cases, filaments are forming during switching and both destructive and non-destructive filaments can be distinguished. Understanding the temporal evolution and the movement of filaments is the key to decide whether a filament will become destructive or not.

ACKNOWLEDGEMENT

The authors would like to thank G. Wachutka for many valuable discussions.

REFERENCES

[1] J. Lutz, H. Schlangenotto, U. Scheuermann, R. De Doncker, "Semiconductor Power Devices" Springer Heidelberg, Dordrecht, London, New York 2011.

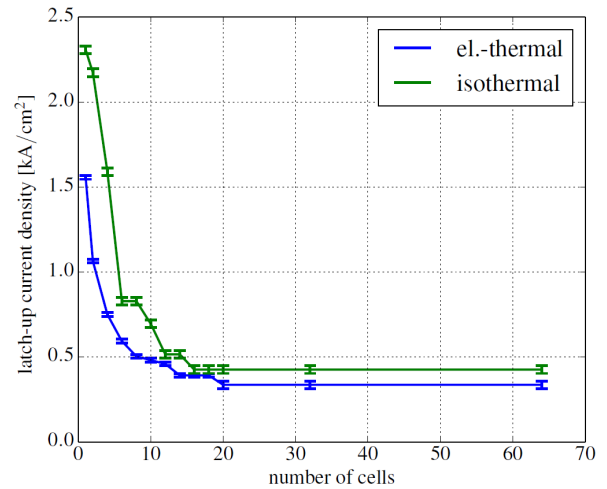


Fig. 6. Latch-up current density as a function of the number of cells in an integrated structure for isothermal and electro-thermal simulations. (From [15])

[2] H.-J. Schulze, F.-J. Niedernostheide, F. Pfirsch, R. Baburske, "Limiting Factors of the Safe Operating Area for Power Devices" *IEEE Trans. Electron Device*, vol. 60, pp 551-562, 2013

[3] M. Chen, J. Lutz, H. P. Felsl, H.-J. Schulze, "A diode structure with anode side buried p doped layers for damping of dynamic avalanche" *Proc. ISPSD*, 2007, pp. 141-144.

[4] M. Pfaffenlehner, H.P. Felsl, F.-J. Niedernostheide, F. Pfirsch, H.-J. Schulze, R. Baburske, J. Lutz, "Optimization of diodes using the SPEED concept and CIBH" *Proc. ISPSD*, 2011, pp. 108-111.

[5] R. Baburske, F.-J. Niedernostheide, E. Falck, J. Lutz, H.-J. Schulze, J. Bauer, "Destruction behavior of power diodes beyond the SOA limit" *Proc. ISPSD*, 2012, pp. 365-368.

[6] T. Raker, H.P. Felsl, F.-J. Niedernostheide, F. Pfirsch, and H.-J. Schulze, "Limits of strongly punch-through designed IGBTs" *Proc. ISPSD*, 2011, pp. 100-104.

[7] P. Rose, D. Silber, A. Porst, F. Pfirsch, "Investigations on the stability of dynamic avalanche in IGBTs" *Proc. ISPSD*, 2002, pp. 165-168.

[8] M. Riccio, A. Irace, G. Breglio, P. Spirito, E. Napoli, Y. Mizuno, "Electro-thermal instability in multi-cellular Trench-IGBTs in avalanche condition: experiments and simulations" *Proc. ISPSD*, 2011, pp. 124-127.

[9] T. Shoji, M. Ishiko, K. Ueta, T. Fukami, and K. Hamada, "Investigation of current filamentation of IGBTs under unclamped inductive switching conditions" *Proc. ISPSD*, 2005, pp. 227-230.

[10] A. Kopta, M. Rahimo, U. Schlapbach, "Limitation of the short-circuit ruggedness of high-voltage IGBTs" *Proc. ISPSD*, 2009, pp. 33-36.

[11] C. Weiß, S. Aschauer, G. Wachutka, A. Härtl, F. Hille, and F. Pfirsch, "Numerical analysis of cosmic radiation-induced failures in power diodes" *Proc. ESSDERC*, 2011, pp. 355-358.

[12] R. Baburske, J. Lutz, H.-J. Schulze, F.-J. Niedernostheide, "Analysis of the destruction mechanism during reverse-recovery of power diodes" *Proc. ISPS*, 2010, pp. 47-54.

[13] J. Lutz, R. Baburske, M. Chen, B. Heinze, M. Domeij, H. P. Felsl, H.-J. Schulze, "The nn^+ -junction as the key to improved ruggedness and soft recovery of power diodes," *IEEE Trans. Electron Devices*, vol. 56, pp 2825-2832, 2009.

[14] C. Töchterle, F. Pfirsch, C. Sandow, G. Wachutka, "Analysis of the latch-up process and current filamentation in high-voltage trench IGBT cell arrays", *Proc. SISPAD*, 2013, pp. 296-299

[15] C. Töchterle, F. Pfirsch, C. Sandow, G. Wachutka, "Evolution of current filaments limiting the safe-operating area of high-voltage trench-IGBTs" *Proc. ISPSD* 2014, in print